Journal of Biomolecular NMR, 1 (1991) 13–22
ESCOM

J-Bio NMR 002

Stereospecific assignment of β-methylene protons in larger proteins using 3D ^{15}N-separated Hartmann-Hahn and ^{13}C-separated rotating frame Overhauser spectroscopy

G. Marius Clore, Ad Bax and Angela M. Gronenborn

Laboratory of Chemical Physics, Building 2, National Institute of Diabetes and Digestive and Kidney Diseases, National Institutes of Health, Bethesda, MD 20892, U.S.A.

Received 22 November 1990
Accepted 2 January 1991

Keywords: Stereospecific assignment; 3D NMR; Heteronuclear NMR; Hartmann-Hahn; ROE

SUMMARY

$^3J_{\alpha\beta}$ coupling constants and complementary nuclear Overhauser data on the intraresidue $C^\alpha H$-$C^\beta H$ distances form an essential part of the data needed to obtain stereospecific assignments of β-methylene protons in proteins. In this paper we show that information regarding the magnitude of the $^3J_{\alpha\beta}$ coupling constants can be extracted from a semi-quantitative interpretation of relative peak intensities in a 3D ^{15}N-separated ^{1}H-^{1}H Hartmann-Hahn ^{1}H-^{15}N multiple quantum coherence (HOHAHA-HMQC) spectrum. In addition, we demonstrate that reliable information on the intraresidue $C^\alpha H$-$C^\beta H$ distances, free of systematic errors arising from spin diffusion, can be obtained from a 3D ^{13}C-separated ^{1}H-^{1}H rotating frame Overhauser effect ^{1}H-^{13}C multiple quantum coherence (ROESY-HMQC) spectrum. The applicability of these experiments to larger proteins is illustrated with respect to interleukin-1β, a protein of 153 residues and 17.4 kDa molecular weight.

INTRODUCTION

It has recently been demonstrated that the precision and accuracy of three-dimensional protein structures determined by NMR is significantly improved by making use of stereospecific assignments of β-methylene protons and χ_1 side-chain torsion angle restraints (Driscoll et al., 1989a, b; Kraulis et al., 1989; Güntert et al., 1989; Qian et al., 1989; Clore et al., 1990a, 1991; Omichinski et al., 1990; Dyson et al., 1990; Forman-Kay et al., 1991). These can be obtained from an analysis

Abbreviations: IL-1β, interleukin-1β; NOE, nuclear Overhauser effect; ROE, rotating frame Overhauser effect; HOHAHA, homonuclear Hartmann-Hahn spectroscopy; NOESY, nuclear Overhauser enhancement spectroscopy; ROESY, rotating frame Overhauser spectroscopy; HMQC, heteronuclear multiple quantum coherence spectroscopy.

of $^3J_{\alpha\beta}$ coupling constants and intra-residue nuclear Overhauser effects (NOEs) involving the NH, $C^{\alpha}H$ and $C^{\beta}H$ protons (Wagner et al., 1987). This procedure works most efficiently and reliably when combined with a systematic conformational grid search, particularly if the above data are supplemented by $^3J_{HN\alpha}$ coupling constants and interresidue sequential NOEs involving the NH, $C^{\alpha}H$ and $C^{\beta}H$ protons (Kraulis et al., 1989; Güntert et al., 1989; Nilges et al., 1990). For proteins of less than 100 residues these parameters can readily be derived from 2D E.COSY type spectra (Griesinger et al., 1982; Mueller, 1987) and NOESY (Jeener et al., 1979) spectra. The application of such 2D methods to larger proteins is rendered problematic on two counts. First, it is often difficult to measure the $^3J_{\alpha\beta}$ couplings and NOE intensities from 2D spectra owing to extensive spectral overlap. Second, the determination of correct relative intraresidue distances between the $C^{\alpha}H$ and $C^{\beta}H$ protons which yields information complementary to the $^3J_{\alpha\beta}$ couplings, may be obscured by spin diffusion.

In this paper we demonstrate that information regarding the relative magnitude of the $^3J_{\alpha\beta}$ coupling constants, which is all that is required for the purposes of stereospecific assignments, can be extracted from a semi-quantitative interpretation of relative peak intensities in a 3D ^{15}N-separated ^1H-^1H Hartmann-Hahn (HOHAHA) spectrum. Second, we show that reliable estimates of relative distances involving the $C^{\alpha}H$ and $C^{\beta}H$ protons can be derived from a 3D ^{13}C-separated ^1H-^1H rotating frame Overhauser (ROESY) spectrum. These experiments are applied to interleukin-1β (IL-1β), a protein of 153 residues and 17.4 kDa, which plays an important role in the immune system (Oppenheim et al., 1976).

EXPERIMENTAL

Sample preparation and NMR spectroscopy

IL-1β was produced and purified as described previously (Wingfield et al., 1986; Gronenborn et al., 1986). Uniform (> 95%) ^{15}N and/or ^{13}C labeled protein was obtained by growing the *Escherichia coli* strain on minimal medium with $^{15}NH_4Cl$ and/or $^{13}C_6$-glucose (MSD Isotopes) as sole nitrogen and carbon sources respectively (Driscoll et al., 1990a; Clore et al., 1990b). Two samples were used: one uniformly labeled with ^{15}N, the other with both ^{15}N and ^{13}C. All experiments were recorded on 1.7 mM protein in 150 mM phosphate buffer pH 5.2 at 36 °C in either 90% H_2O/10% D_2O (for the 3D ^1H-^{15}N HOHAHA-HMQC experiment) or 99.996% D_2O (for the 3D ^1H-^{13}C ROESY-HMQC experiment). The 3D spectra were obtained on a Bruker AM-600 spectrometer, operating in 'reverse' mode.

In both 3D heteronuclear separated experiments described in this paper, ^1H chemical shifts evolve during the evolution period t_1 and are detected during the acquisition period t_3. Heteronuclear multiple quantum coherence (Mueller, 1979; Bax et al., 1983) is generated during the period t_2 and subsequently converted back into transverse ^1H magnetization so that at the end of the t_2 period ^1H magnetization is modulated by the shift of its directly attached heteronucleus (^{13}C or ^{15}N depending on the experiment).

The pulse sequence for the ^{15}N-separated HOHAHA-HMQC spectrum is as follows:

$$\begin{array}{lcccccccccccc} ^1H & 90_{\psi 1} & - & t_1 & - & TP_y & - & [DIPSI\text{-}2_x & - & 60_y]_n & - & TP_y & - \\ ^{15}N & & & & & & & & & & & & \\ \end{array}$$

$$\begin{array}{lcccccccccccc} 90_x & - & \tau & - & 90_{\phi 1} & - & \Delta & - & 180_x & - & \Delta & - & Acq \\ & & & & & & & & & & & & \\ \end{array}$$

$$\begin{array}{lcccccccccccc} & & & & & & & & & & & & \\ Dec & & & & & & 90_{\psi 2} & - & t_2/2 & - & -t_2/2 & - & 90_{\phi 2} & - & Dec \end{array} \quad (1)$$

with phase cycling $\psi 1 = x, -x$; $\phi 2 = 2(x), 2(-x)$; $\phi 1 = 4(x), 4(y), 4(-x), 4(-y)$; Acq = x, 2(−x), x, −y, 2(y), −y, −x, 2(x), −x, y, 2(−y), y. The delay τ was set to half the DIPSI-2 mixing time to minimize ROE effects (Marion et al., 1989a); and the delay Δ was set to 4.5 ms, slightly less than $1/(2J_{NH})$. The duration of the DIPSI-2 mixing time was 30.7 ms. The trim pulse TP was set to 800 μs. ^{15}N decoupling (Dec) during the t_1 evolution period and the acquisition time was achieved with random GARP modulation (Shaka et al., 1985). Water suppression was achieved by weak coherent presaturation during the relaxation delay. The spectrum was recorded with 128 complex (t_1) × 32 complex (t_2) × 1024 real (t_3) points. The spectral widths in the ^{1}H(F_1), ^{15}N(F_2) and ^{1}H(F_3) dimensions were 11.26, 26.0 and 13.89 ppm, respectively, and the incremental delays Δt_1 and Δt_2 were 148 and 632 μs, respectively. The ^{1}H and ^{15}N carrier frequencies were placed at 4.67 and 121 ppm, respectively. The field strengths for the ^{1}H and ^{15}N pulses were 9.43 and 3.97 kHz, respectively, and the field strength used for ^{15}N GARP decoupling was 1 kHz.

The pulse sequence for the ^{13}C-separated ROESY-HMQC spectrum is as follows:

$$\begin{array}{lccccccc} ^1\mathrm{H} & 90_{\psi 1} - t_1/2 - & & - t_1/2 - \mathrm{SL}_{\phi 2} - \Delta - & & 180_{\phi 3} & \Delta - \mathrm{Acq} & \\ ^{13}\mathrm{C} & & 180_{\phi 1} & & 90_{\psi 2} - t_2/2 - & - t_2/2 - 90_x - & 90_x 90_{\phi 4} \mathrm{Dec} & (2) \end{array}$$

with phase cycling: $\psi 1 = 4(x), 4(y)$; $\psi 2 = x, -x$; $\phi 1 = 4(x), 4(-x)$; $\phi 2 = 4(y), 4(-x), 4(-y), 4(x)$; $\phi 3 = 2(x), 2(y), 2(-y), 2(x), 2(-x), 2(-y), 2(y), 2(-x)$; $\phi 4 = 8(x), 8(-x)$; Acq = x, 2(−x), x, y, 2(−y), y. The ^{13}C $180_{\phi 1}$ pulse is a composite 180° pulse of the type $90_x 180_y 90_x$. The delay Δ was set to 3 ms, slightly less than $1/(2J_{CH})$. ^{13}C decoupling during the acquisition period was achieved using coherent GARP decoupling, and the ^{13}C $90_x 90_{\phi 4}$ pulse pair, at the beginning of acquisition prior to the start of decoupling, reduces the intensity of modulation side bands (Bax et al., 1990). The ROESY spin lock SL was applied for 22 ms. The spectrum was recorded with 128 complex (t_1) × 32 complex (t_2) × 1024 real (t_3) points. The spectral widths in the ^{1}H(F_1), ^{13}C(F_2) and ^{1}H(F_3) dimensions were 8.78, 20.71 and 18.11 ppm, respectively, and the incremental delays Δt_1 and Δt_2 were 190 and 320 μs, respectively. The ^{1}H and ^{13}C carrier frequencies were placed at 7 and 43 ppm, respectively. The ^{1}H carrier was placed to low field of the $C^\alpha H$ resonances to avoid any artifacts arising from Hartmann-Hahn transfer between $C^\alpha H$ and $C^\beta H$ protons in cases where the matching for this process is near perfect (i.e. when the two resonances have equal but opposite offsets from the carrier frequency). Therefore, carrier shifting in F_1 was required when using an 8.78 ppm F_1 spectral width. This was achieved by applying a linear phase shift correction of 18386° to the time domain data in t_2 during processing, thereby shifting the carrier in F_1 to 3.5 ppm (this phase correction is given by ($\Delta\nu$/SW) × number of complex points × 360°, where SW is the spectral width and $\Delta\nu$ is the required carrier shift, Bax et al., 1983; Bothner-By and Dadok, 1987). The field strengths for the ^{1}H and ^{13}C pulses were 8.33 and 14.5 kHz, respectively, and the field strength used for ^{13}C GARP decoupling was 3.85 kHz.

Quadrature detection in the indirectly detected dimensions was achieved using the TPPI-States method (Marion et al., 1989b). This involves incrementing the phases of $\psi 1$ and $\psi 2$ independently by 90° to generate complex data in the t_1 and t_2 dimensions, respectively. In addition, every time t_1 is incremented the receiver phase and $\psi 1$ are also incremented by 180°, and similarly for the receiver phase and $\psi 2$ in the case of the t_2 dimension.

The spectra were processed on a Sun Sparc Workstation using simple in-house routines (Kay et al., 1989) for the Fourier transform in F_2, together with the commercially available software pack-

age NMR2 (New Methods Research Inc., Syracuse, N.Y.) for processing the F_1-F_3 planes. Zero-filling (once in each dimension) was employed to yield final absorptive spectra of 256 × 64 × 1024 data points. A regular 60°-shifted sine bell window function was applied in the F_1 and F_3 dimensions, while a doubly shifted sine bell function, shifted by 60° at the beginning of the window and 10° at the end of the window was used in the F_2 dimension (Kay et al., 1989).

RESULTS AND DISCUSSION

Analysis of extensively refined high-resolution X-ray structures in the Brookhaven Protein Data Bank has shown that 95% of all χ_1 side-chain torsion angles lie within ±15° of the staggered rotamer conformations (60°, −60° and 180°), and that improvements in refinement go hand in hand with more and more χ_1 angles approaching the ideal staggered rotamer conformations (Ponder and Richards, 1987; McGregor et al., 1987; Nilges et al., 1990). Although at present there is not an equal number of solution structures available which could be used as a data base for a similar analysis, the high-resolution solution NMR structures determined to date indicate that two situations are predominantly observed. The side-chain is either well ordered, in which case the χ_1 angle is also close to one of the three staggered rotamer conformations, or it is disordered (Wagner et al., 1987; Kraulis et al., 1989; Clore et al., 1990a, 1991; Forman-Kay et al., 1991). The latter also includes cases where two or three of the staggered rotamer conformations coexist in rapid equilibrium. If both $^3J_{\alpha\beta}$ coupling constants are small (< 4 Hz), χ_1 must lie around 60°. If one of the two $^3J_{\alpha\beta}$ coupling constants is large (> 10 Hz), then the other must be small (< 4 Hz), and χ_1 has a value close to either −60° or 180°. The latter two possibilities can then be distinguished on the basis of either the relative intensities of the intraresidue NH-C$^\beta$H NOEs (Wagner et al., 1987) or the size of the heteronuclear $^3J_{N\beta}$ couplings (Bystrov, 1976). Finally, if the side-chain is disordered, the $^3J_{\alpha\beta}$ couplings are approximately equal with values ranging from 6-8 Hz, as are the approximate relative intensities of the various NOEs involving the two β-methylene protons. Given these observations, it follows that a qualitative estimate of the magnitude of the $^3J_{\alpha\beta}$ coupling constants is sufficient for the purposes of stereospecific assignment, particularly when systematic conformational grid search procedures are used (Güntert et al., 1989; Nilges et al., 1990).

In small proteins, $^3J_{\alpha\beta}$ coupling constants can be measured most accurately from the displacement caused by the passive J coupling in well-resolved C$^\alpha$H-C$^\beta$H cross peaks in correlated spectra with reduced multiplets, such as E.COSY (Griesinger et al., 1982), β-COSY (Bax and Freeman, 1981), PE.COSY (Mueller, 1987; Bax and Lerner, 1988) and z.COSY (Oschkinat et al., 1986). For larger proteins, the increased line width together with extensive spectral overlap may frequently make it impossible to extract these couplings with confidence. Although in principle one might expect that ^{13}C-separated 3D E.COSY-type spectra could alleviate at least the overlap problem, in practice, the introduction of ^{13}C severely broadens the ^{1}H resonances and makes this type of approach impractical. Other approaches, using either long range heteronuclear couplings (Cowburn et al., 1983) or passive couplings measured in isotopically enriched proteins can also be used for this purpose (Montelione et al., 1989; Wider et al., 1989) but have not yet gained widespread popularity for a number of technical reasons. Fortunately, as will be shown below, a qualitative knowledge of the relative sizes of the $^3J_{\alpha\beta}$ couplings can be readily derived from the intensities of the well-resolved HN-C$^\beta$H cross peaks in a 3D ^{15}N-separated HOHAHA-HMQC spectrum recorded with a short mixing period.

Cross-peak intensities in isotropic mixing experiments depend on the rate at which magnetization flows through a J-coupled spin system during the mixing period. This rate depends not only on the topology of the spin system and on the size of the pertinent J couplings, but also on the quality of the isotropic mixing scheme used. For the newer isotropic mixing schemes of the DIPSI variety, off-resonance effects are minimal, and near-ideal mixing can be obtained over a substantial bandwidth (Shaka et al., 1988; Rucker and Shaka, 1988). Cross-peak intensities also depend on the relaxation rates of the originating and destination protons, as well as on the other proton spins involved in the transfer pathway. These relaxation rates are generally only known with a low degree of accuracy, and may vary substantially for amino acids of the same type at different locations in the protein. This diversity in relaxation rates makes it difficult to fit in a rigorous manner the cross-peak intensities observed in HOHAHA type spectra to magnetization transfer curves that can be calculated for each of the amino acids (Cavanagh et al., 1990). However, a good estimate of the relative size of the J coupling between the $C^{\alpha}H$ and $C^{\beta 2}H/C^{\beta 3}H$ protons can be obtained from relative intensities of the HN-$C^{\beta 2}H$ and HN-$C^{\beta 3}H$ cross peaks, assuming that the two β-methylene protons have similar relaxation times. Since relaxation of the β-methylene protons is typically dominated by their geminal dipolar interaction, this assumption is perfectly reasonable. Thus, if only the relative amount of HN-$C^{\beta 2}H$ and HN-$C^{\beta 3}H$ magnetization transfer is of interest, the magnetization from the HN to the $C^{\beta}H$ protons may be calculated neglecting relaxation, since relaxation of the HN and $C^{\alpha}H$ protons has the same effect on both magnetization transfers.

Figure 1 shows the transfer of magnetization from the HN to the $C^{\beta}H$ protons as a function of mixing time for a residue with two non-equivalent $C^{\beta}H$ protons. The curves are calculated with coupling constants of $^3J_{HN\alpha} = 5$ Hz or 10 Hz, $^3J_{\alpha\beta 3} = 4$ Hz and $^3J_{\alpha\beta 2} = 11$ Hz. As expected, it is seen that for short mixing times transfer to the $C^{\beta 2}H$ proton is much larger than transfer to the $C^{\beta 3}H$ proton. Figure 2 plots the ratio of the two cross-peak intensities as a function of mixing time. This ratio can be slightly reduced if there are other protons coupled to the $C^{\beta}H$ protons. The dashed lines in both Figs. 1 and 2 correspond to a 'worst case scenario' where a single $C^{\gamma}H$ proton has a large coupling (11 Hz) to $C^{\beta 2}H$ and a small coupling (4 Hz) to $C^{\beta 3}H$. As can be seen in Fig.

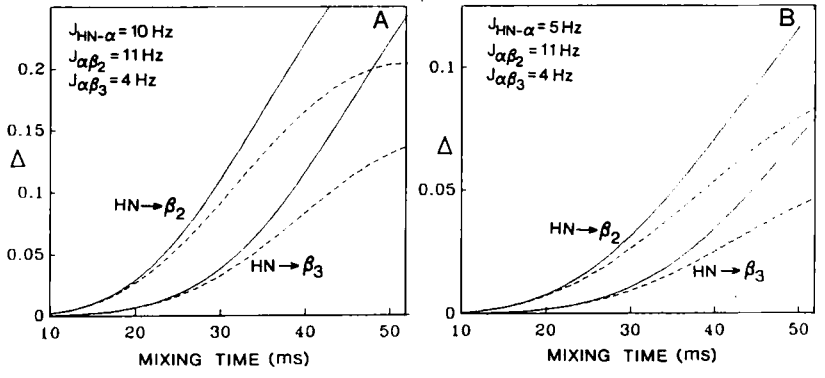

Fig. 1. Fraction of magnetization, Δ, transferred from the HN to the $C^{\beta 2}H$ and $C^{\beta 3}H$ protons as a function of the duration of isotropic mixing for (A) $^3J_{HN\alpha} = 10$ Hz and (B) $^3J_{HN\alpha} = 5$ Hz. For both cases $^2J_{\beta 2\beta 3} = -14$ Hz. Ideal isotropic mixing is assumed and the fractions are calculated in the absence of relaxation. Relaxation attenuates the HN→$C^{\beta 2}H$ and HN→$C^{\beta 3}H$ magnetization transfer to the same extent. The solid lines correspond to a spin system without $C^{\gamma}H$ protons; the dashed lines corresponds to a spin system with a single $C^{\gamma}H$ proton with $^3J_{\beta 2\gamma} = 11$ Hz and $^3J_{\beta 3\gamma} = 4$ Hz.

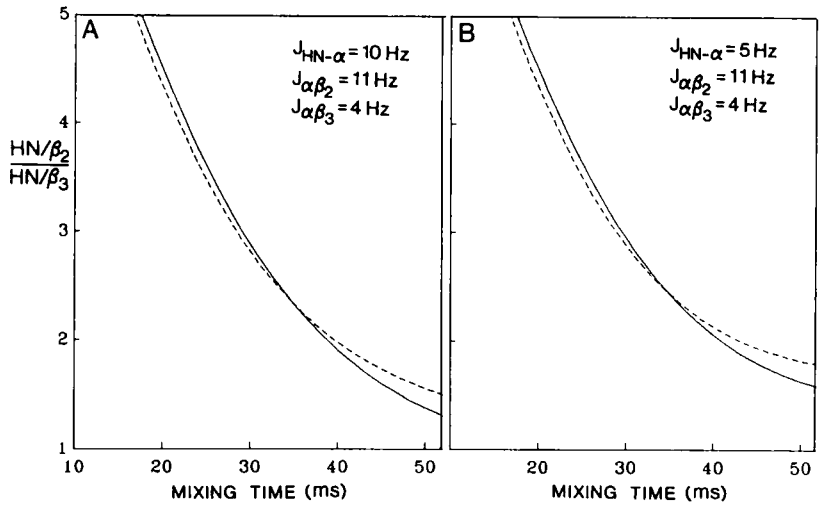

Fig. 2. Ratio of the HN-C$^{\beta 2}$H and HN-C$^{\beta 3}$H cross-peak intensities as a function of isotropic mixing duration for (A) $^3J_{HN\alpha}$ = 10 Hz, and (B) $^3J_{HN\alpha}$ = 5 Hz. The solid lines correspond to a spin system without C$^\beta$H protons, the dashed lines correspond to a spin system with a single C$^\beta$H proton with $^3J_{\beta 2\gamma}$ = 11 Hz and $^3J_{\beta 3\gamma}$ = 4 Hz.

2, this reduces the cross-peak ratio slightly for short mixing times (< 35 ms), although the absolute HN-C$^\beta$H cross-peak intensities can be affected quite significantly (Fig. 1).

Distinguishing between amino acids with free rotation about the C$^\alpha$-C$^\beta$ bond and amino acids with the $\chi_1 = 60^\circ$ rotamer that puts both methylene protons in gauche positions with respect to the C$^\alpha$H proton, requires a comparison of the HN-C$^\alpha$H and HN-C$^\beta$H cross-peak intensities. Because the transverse relaxation rates of the C$^\alpha$H and C$^\beta$H protons may differ substantially, this type of semi-quantitative interpretation of cross-peak ratios is less straightforward than the case discussed above. In the case of a fixed rotamer with $\chi_1 = 60 \pm 30^\circ$, both $^3J_{\alpha\beta}$ couplings are less than about 4 Hz, whereas in the case of free rotation, the couplings are between 6 and 8 Hz. Thus, stronger HN-C$^\beta$H cross peaks are expected for the free-rotation case relative to a fixed $\chi_1 \sim 60^\circ$ rotamer. These cross-peak intensities, however, also depend strongly on the size of the $^3J_{HN\alpha}$ coupling. Figure 3 shows the ratio of the intensities expected for the HN-C$^\beta$H and HN-C$^\alpha$H cross peaks for both 4 Hz and 7 Hz $^3J_{\alpha\beta}$ couplings, assuming identical relaxation times for all spins involved. In the case of free rotation, the relaxation time of the C$^\beta$H protons is expected to become longer relative to the case of a fixed rotamer, which would increase the C$^\beta$H/HN:C$^\alpha$H/HN cross-peak ratio to an even larger value compared to the fixed $\chi_1 \sim 60^\circ$ rotamer. The C$^\beta$H/HN:C$^\alpha$H/HN cross-peak ratios shown in Fig. 3 are drawn for the $^3J_{HN\alpha}$ coupling of 7 Hz but depend only weakly on the size of this coupling provided it is in the 4-10 Hz range.

Figure 4 illustrates the HN-C$^\alpha$H and HN-C$^\beta$H cross peaks for some typical residues obtained for the 3D ^{15}N-separated HOHAHA-HMQC spectrum of IL-1β recorded with a duration of 30.7 ms for the DIPSI-2 mixing sequence. In the case of $\chi_1 = -60^\circ$ (Fig. 4A) or $\chi_1 = 180^\circ$ (Fig. 4B), it is generally the case that only one of the two possible HN-C$^\beta$H cross peaks is observed, corresponding to the C$^\beta$H proton with the larger $^3J_{\alpha\beta}$ coupling (i.e. C$^{\beta 2}$H in the case of $\chi_1 = -60^\circ$ and C$^{\beta 3}$H in the case of $\chi_1 = 180^\circ$). Occasionally both HN-C$^\beta$H cross peaks can be observed (e.g. Asp-142 in Fig. 4A), but in such cases one of the cross peaks is much stronger than the other. For those

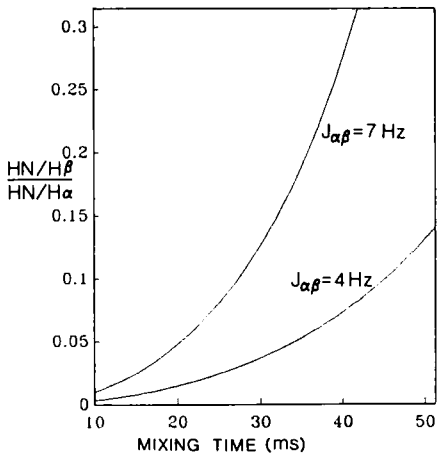

Fig. 3. Ratio of the HN-C$^{\alpha}$H and HN-C$^{\beta}$H cross-peak intensities when both C$^{\beta}$H methylene protons have identical couplings to the C$^{\alpha}$H proton. The HN-C$^{\beta}$H cross-peak intensity corresponds to a single C$^{\beta}$H proton (i.e. if the two C$^{\beta}$H protons have degenerate chemical shifts the cross-peak ratio will be twice that shown in the graph). The cross-peak ratios have been calculated with $^{3}J_{HN\alpha}$ = 7 Hz and no C$^{\alpha}$H protons.

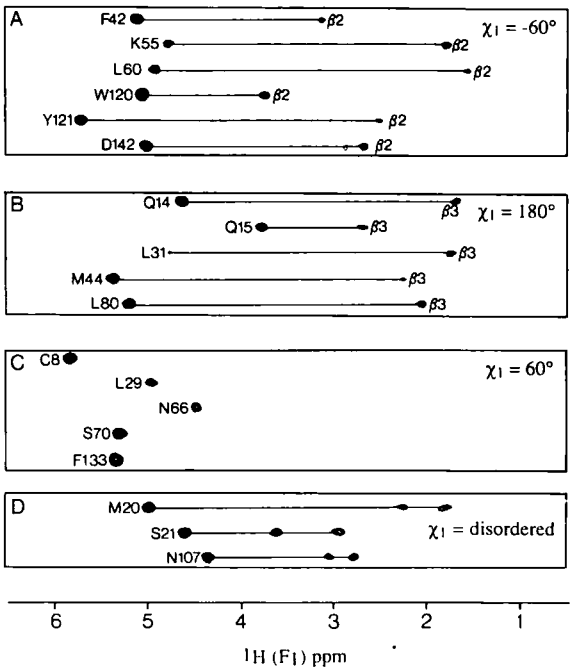

Fig. 4. Composite of amide strips taken from the 3D ^{15}N-separated HOHAHA-HMQC spectrum of ^{15}N labeled IL-1β recorded with a 30.7 ms mixing time showing NH-C$^{\alpha}$H and NH-C$^{\beta}$H cross peaks for a number of residues. Examples of residues with $\chi_1 = -60$, 180° and 60° are shown in (A), (B) and (C), respectively, while residues with disordered χ_1 conformations are shown in (D). The strips were extracted from the 3D spectrum as described by Driscoll et al. (1990a). The assignments are from Driscoll et al. (1990a) and Clore et al. (1990c).

residues with $\chi_1 = 60°$ (Fig. 4C), where both $^{3}J_{\alpha\beta}$ couplings are small, no relayed HN-C$^{\beta}$H cross peaks are observed. Finally, for those residues with disordered χ_1 conformations (Fig. 4D), both HN-C$^{\beta}$H cross peaks are seen with approximately equal intensity. It is also important to point out that the qualitative results obtained from this spectrum are in complete agreement with the quantitative $^{3}J_{\alpha\beta}$ couplings measured from a 2D PE.COSY spectrum for all residues where the C$^{\alpha}$H-C$^{\beta}$H cross peaks were sufficiently resolvable.

In principle, the C$^{\alpha}$H-C$^{\beta}$H NOE cross-peak intensities recorded with a short mixing time provide information that is of the same nature as the $^{3}J_{\alpha\beta}$ couplings discussed above. A rotamer with one of the C$^{\beta}$H protons trans relative to the C$^{\alpha}$H proton is expected to show a much stronger NOE to the gauche C$^{\beta}$H proton than to the trans one, thus allowing $\chi_1 = 60°$ and $\chi_1 = -60°$ or 180° to be distinguished. In practice, it is difficult to obtain a 3D ^{13}C-separated NOESY spectrum with a short enough mixing time to avoid spin diffusion. Such 3D spectra recorded with very short mixing times have intense diagonal resonances with substantial amounts of t_1-noise associated with these intense resonances, thus obscuring many of the weaker cross peaks (unpublished observations). Here we demonstrate that a ^{13}C-separated ROESY experiment is a feasible technique

and a useful alternative to the short mixing time NOESY. In the rotating frame, the Overhauser effect (ROE) is positive for all values of the molecular correlation time τ_c (Bothner-By et al., 1984). Therefore, indirect ROE contributions are of opposite sign relative to direct ROE effects in the case of one intervening spin (Bax et al., 1986). Positive indirect effects involving an even number of intermediate spins are generally unobservable because positive and negative contributions tend to cancel one another. Thus, ROESY spectra recorded with reasonably long mixing periods still give a faithful representation of internuclear distance both for small proteins and oligonucleotides (Bauer et al., 1990) and for larger proteins such as IL-1β (Clore et al., 1990c). When setting up the ROESY experiment, we determine the approximate average value of the spin-locked relaxation time $T_{1\rho}$, and use this value for the mixing time duration in the ROESY experiment, thereby optimizing the signal-to-noise ratio. For our present example, namely IL-1β, this duration was 22 ms. Diagonal resonances recorded with this mixing time are attenuated significantly, and reasonably strong cross peaks can be readily observed. As a consequence of the short mixing time, however, interproton distances larger than about 3.5 Å do not give rise to observable ROE cross peaks.

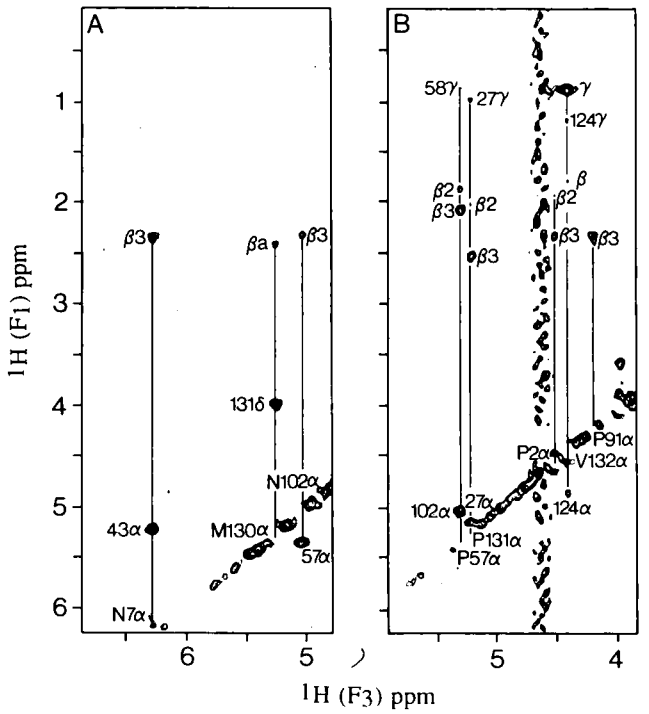

Fig. 5. Two ^{1}H(F_1)-^{1}H(F_3) planes at different ^{13}C frequencies of the 3D ^{13}C-separated ROESY-HMQC spectrum of ^{13}C,^{15}N labeled IL-1β recorded with a 22 ms mixing time. (A) ROEs to the C$^\alpha$H protons of Asn-7, Asn-102 and Met-130 at δ^{13}C = 51.4 ($\pm$nSW) ppm (the spectral width SW is 20.71 ppm). Only positive levels are shown and diagonal resonances are therefore not observed. In the case of Asn-7 and Asn-102, $\chi_1 \sim -60°$, while for Met-130 we were unable to make the distinction between $\chi_1 \sim -60°$ and $\chi_1 \sim 180°$. Note, however, that for Met-130, a ROE between the C$^\alpha$H proton and only one of the two C$^\beta$H protons, namely the low-field C$^{\beta_2}$H, is observed, indicative of an ordered conformation with $\chi_1 \sim -60°$ or $-180°$. (B) ROEs to the C$^\alpha$H protons of Pro-2, Pro-57, Pro-91, Pro-131 and Val-132 at δ^{13}C = 61.9 ($\pm$nSW) ppm. Note that in addition to intraresidue ROEs, a number of both short and long range interresidue ROEs are observed in both slices. The assignments are from Clore et al. (1990c).

Figure 5 illustrates some typical $^{1}H(F_1)$-$^{1}H(F_3)$ slices at different $^{13}C(F_2)$ frequencies of the ^{13}C-separated ROESY-HMQC spectrum of IL-1β. In the case of $\chi_1 = -60^\circ$ or 180° (e.g Asn-7, Asn-102 and Met-130 in Fig. 5A) it is clear that one of the $C^\alpha H$-$C^\beta H$ ROEs is much stronger than the other, while for $\chi_1 = 60^\circ$, the two ROEs are strong and of approximately equal intensity (data not shown). In addition, the relative distances between the $C^\alpha H$ and $C^\beta H$ protons in proline residues where $\chi_1 = -30$ to $+30^\circ$, is readily ascertained. This provides unambiguous data on the stereospecific assignment of the $C^\beta H$ methylene protons of proline, as the $C^\alpha H$-$C^{\beta 3} H$ distance is usually shorter and can never be longer than the $C^\alpha H$-$C^{\beta 2} H$ distance (Clore et al., 1986). This is clearly seen in Fig. 5B which displays ROEs involving the $C^\alpha H$ and $C^\beta H$ protons of four proline residues, Pro-2, Pro-57, Pro-91 and Pro-131. For these four proline residues (as well as for all the other prolines in IL-1β), either only a ROE to a single $C^\beta H$ proton is observed (e.g. Pro-91), or the ROE to one of the $C^\beta H$ protons is much stronger than that to the other $C^\beta H$ proton (e.g. Pro-2, Pro-57 and Pro-131), making the distinction of the $C^{\beta 3} H$ and $C^{\beta 2} H$ resonances simple. Also of interest in the 3D ^{13}C-separated ROESY spectrum is the observation of a number of interresidue ROEs both short range (e.g. between Met-130 $C^\alpha H$ and Pro-131 $C^\delta H$ in Fig. 5A and between Pro-57 $C^\alpha H$ and Val-58 $C^\gamma H$ in Fig. 5B) and long range (e.g. between Asn-7 $C^\alpha H$ and Ser-43 $C^\alpha H$, Pro-57 $C^\alpha H$ and Asn-102 $C^\alpha H$, Pro-131 $C^\alpha H$ and Lys-27 $C^\alpha H$, Pro-131 $C^\alpha H$ and Lys-27 $C^\gamma H$, Val-132 $C^\alpha H$ and Thr-124 $C^\alpha H$, and Val-132 $C^\alpha H$ and Thr-124 $C^\gamma H$).

Using the data from spectra such as those described above, together with $^{3}J_{HN\alpha}$ couplings obtained by Driscoll et al. (1990b) from an HMQC-J spectrum (Kay and Bax, 1989), and relative distance restraints for the intra- and sequential interresidue $C^\alpha H$-NH and $C^\beta H$-NH NOEs derived from a short-mixing-time 3D ^{15}N-separated NOESY spectrum, we were able to obtain, using the conformational grid search program STEREOSEARCH (Nilges et al., 1990), stereospecific assignments and ϕ, ψ and χ_1 torsion angle restraints for 81 of the 121 residues (i.e. 67% of the residues) in IL-1β with C^β methylene protons (Clore et al., 1991). For the remainder, either $\chi_1 = -60^\circ$ could not be distinguished from $\chi_1 = 180^\circ$, or the β-methylene protons have degenerate shifts, or the STEREOSEARCH program was unable to find a combination of ϕ, ψ and χ_1 angles compatible with the NMR data. The latter is indicative of multiple side-chain orientations. In this respect, it is interesting to note that nearly all of the residues for which no stereospecific assignments could be made are located on the protein surface.

ACKNOWLEDGEMENTS

This work was supported by the AIDS Directed Anti-Viral Program of the Office of the Director of the National Institutes of Health. Figures 1-3 were derived from calculations made with the generalized NMR simulation program ANTIOPE which was kindly provided to us by Prof. J.S. Waugh (MIT). We thank Dr. Mitsu Ikura for many useful and stimulating discussions.

REFERENCES

Bauer, C.J., Frenkiel, T.A. and Lane, A.N. (1990) *J. Magn. Reson.*, **87**, 144-152.
Bax, A. and Freeman, R. (1981) *J. Magn. Reson.*, **44**, 542-561.
Bax, A. and Davis, D.G. (1985) *J. Magn. Reson.*, **63**, 207-213.
Bax, A. and Lerner, L.E. (1988) *J. Magn. Reson.*, **79**, 429-438.
Bax, A., Griffey, R.H. and Hawkins, B.L. (1983) *J. Magn. Reson.*, **55**, 301-315.

Bax, A., Sklenar, V. and Summers, M.F. (1986) *J. Magn. Reson.*, **70**, 327-331.
Bax, A., Clore, G.M., Driscoll, P.C., Gronenborn, A.M., Ikura, M. and Kay, L.E. (1990) *J. Magn. Reson.*, **87**, 620-627.
Bothner-By, A.A. and Dadok, J. (1987) *J. Magn. Reson.*, **72**, 540-543.
Bothner-By, A.A., Stephens, R.L., Lee, J.T., Warren, C.D. and Jeanloz, R.W. (1984) *J. Am. Chem. Soc.*, **106**, 811-813.
Bystrov, V.F. (1976) *Prog. Nucl. Magn. Reson. Spectrosc.*, **10**, 41-81.
Cavanagh, J., Chazin, W.J. and Rance, M. (1990) *J. Magn. Reson.*, **72**, 540-543.
Clore, G.M., Gronenborn, A.M., Carlson, G. and Meyer, E.F. (1986) *J. Mol. Biol.*, **190**, 259-267.
Clore, G.M., Appella, E., Yamada, M., Matsushima, K. and Gronenborn, A.M. (1990a) *Biochemistry*, **29**, 1689-1696.
Clore, G.M., Bax, A., Driscoll, P.C., Wingfield, P.T. and Gronenborn, A.M. (1990b) *Biochemistry*, **29**, 8172-8184.
Clore, G.M., Bax, A., Wingfield, P.T. and Gronenborn, A.M. (1990c) *Biochemistry*, **29**, 5671-5676.
Clore, G.M., Wingfield, P.T. and Gronenborn, A.M. (1991) *Biochemistry*, **30**, 2315-2323.
Cowburn, D., Live, D.H., Fischman, A.J. and Agosta, W.C. (1983) *J. Am. Chem. Soc.*, **105**, 7435-7442.
Davis, D.G. and Bax, A. (1985) *J. Am. Chem. Soc.*, **107**, 2820-2821.
Driscoll, P.C., Gronenborn, A.M. and Clore, G.M. (1989a) *FEBS Lett.*, **243**, 223-233.
Driscoll, P.C., Gronenborn, A.M., Beress, L. and Clore, G.M. (1989b) *Biochemistry*, **28**, 2188-2198.
Driscoll, P.C., Clore, G.M., Marion, D., Wingfield, P.T. and Gronenborn, A.M. (1990a) *Biochemistry*, **29**, 3542-3556.
Driscoll, P.C., Gronenborn, A.M., Wingfield, P.T. and Clore, G.M. (1990b) *Biochemistry*, **29**, 4668-4682.
Dyson, H.J., Gippert, G.P., Case, D.A., Holmgren, A. and Wright, P.E. (1990) *Biochemistry*, **29**, 4129-4136.
Forman-Kay, J.D., Clore, G.M., Wingfield, P.T. and Gronenborn, A.M. (1991) *Biochemistry*, **30**, 2685-2698.
Griesinger, C., Sørensen, O.W. and Ernst, R.R. (1982) *J. Am. Chem. Soc.*, **104**, 6800-6802.
Gronenborn, A.M., Clore, G.M., Schmeissner, U. and Wingfield, P.T. (1986) *Eur. J. Biochem.*, **161**, 37-43.
Güntert, P., Braun, W., Billeter, M. and Wüthrich, K. (1989) *J. Am. Chem. Soc.*, **111**, 3997-4004.
Jeener, J., Meier, B.H., Bachmann, P. and Ernst, R.R. (1979) *J. Chem. Phys.*, **71**, 4546-4553.
Kay, L.E. and Bax, A. (1989) *J. Magn. Reson.*, **86**, 110-126.
Kay, L.E., Marion, D. and Bax, A. (1989) *J. Magn. Reson.*, **84**, 72-84.
Kraulis, P.J., Clore, G.M., Nilges, M., Jones, T.A., Pettersson, G., Knowles, J. and Gronenborn, A.M. (1989) *Biochemistry*, **28**, 7241-7257.
Marion, D., Driscoll, P.C., Kay, L.E., Wingfield, P.T., Bax, A., Gronenborn, A.M. and Clore, G.M. (1989a) *Biochemistry*, **28**, 6150-6156.
Marion, D., Ikura, M., Tschudin, R. and Bax, A. (1989b) *J. Magn. Reson.*, **85**, 393-399.
McGregor, M.J., Islam, S.A. and Sternberg, M.J.E. (1987) *J. Mol. Biol.*, **198**, 295-310.
Montelione, G.T., Winkler, M.E., Rauenbuehler, P. and Wagner, G. (1989) *J. Magn. Reson.*, **82**, 198-204.
Mueller, L. (1979) *J. Am. Chem. Soc.*, **101**, 4481-4484.
Mueller, L. (1987) *J. Magn. Reson.*, **72**, 191-196.
Nilges, M., Clore, G.M. and Gronenborn, A.M. (1990) *Biopolymers*, **29**, 813-822.
Omichinski, J.G., Clore, G.M., Appella, E., Sakaguchi, K. and Gronenborn, A.M. (1990) *Biochemistry*, **29**, 9324-9334.
Oppenheim, J.J., Kovacs, E.J., Matsushima, K. and Durum, S.K. (1986) *Immunol. Today*, **7**, 45-56.
Oschkinat, H., Pastore, A., Pfändler, P. and Bodenhausen, G. (1986) *J. Magn. Reson.*, **69**, 559-566.
Ponder, J.W. and Richards, F.M. (1987) *J. Mol. Biol.*, **193**, 775-791.
Qian, Y.Q., Billeter, M., Otting, G., Müller, M., Gehring, W.J. and Wüthrich, K. (1989) *Cell*, **59**, 573-580.
Rucker, S.P. and Shaka, A.J. (1988) *Mol. Phys.*, **68**, 509-514.
Shaka, A.J., Lee, C.J. and Pines, A. (1988) *J. Magn. Reson.*, **77**, 274-293.
Wagner, G., Braun, W., Havel, T.F., Schaumann, T., Go, N. and Wüthrich, K. (1987) *J. Mol. Biol.*, **196**, 611-639.
Wider, G., Neri, D., Otting, G. and Wüthrich, K. (1989) *J. Magn. Reson.*, **85**, 426-431.
Wingfield, P.T., Payton, M., Tavernier, J., Barnes, M., Shaw, A., Rose, K., Simona, M.G., Demaczuk, S., Williamson, K. and Dayer, J.M. (1986) *Eur. J. Biochem.*, **160**, 491-497.